Study of "Sticking and restarting phenomenon" in electropneumatic positioning systems

Xavier Brun, Sylvie Sesmat, Daniel Thomasset, Serge Scavarda

STUDY OF 'STICKING AND RESTARTING PHENOMENON' IN ELECTROPNEUMATIC POSITIONING SYSTEMS

Xavier Brun, Sylvie Sesmat, Daniel Thomasset and Serge Scavarda

Laboratoire d'Automatique Industrielle,
http://www-lai.insa-lyon.fr
INSA Lyon, Bâtiment Saint Exupéry, 25 Avenue Jean Capelle, 69621 Villeurbanne, France
Tel: (33) 4 72 43 88 81; fax: (33) 4 72 43 85 35; e-mail : xavier.brun@lai.insa-lyon.fr

Abstract

This paper explains the possible occurrence of the 'sticking and restarting phenomenon' observed with electropneumatic positioning systems. This is carried out from the notion of partial equilibrium, with the analysis of the model which incorporate two parallel phenomena, these are used to generate a pressure force which is subjected to dry friction forces. Also an experimental result has been studied in a particular pressure force plane which shows the origin of the problem more explicitly. The theoretical results give a necessary and sufficient condition for the restarting phenomenon not to occur and, if this condition is not validated, there is an estimation of the restarting time. Understanding this undesirable phenomenon will be the basis for further work which will attempt to find solutions to avoid its occurrence.

1 Introduction

1.1 Background

Servopneumatic positioning systems, which use micro-controllers for data analysis and sensors for closed loop feedback, have begun entering the industry in robotic welding, packaging machinery, food processing, and automotive assembly. The servopneumatic systems, which first reached the market in the early 1990s, provide an alternative to hydraulic cylinders in situations where huge forces are not needed, or where oil leakage is unacceptable. They also offer a less costly alternative to electric servo drives especially where ultra precise positioning capabilities are not required. One of the reasons of the preference for the electrical technology for precise positioning is the possible occurrence of a restarting phenomenon after a sticking stage in the electropneumatic case as illustrated by some experimental results in Fig. 1 (showing only the end of piston displacements). In this paper this occurrence is called the 'sticking and restarting phenomenon' to distinguish it from the well-known stick-slip phenomenon.

This effect truly hinders the industrial development of electropneumatic technology. In fact, the dynamic stage of the positioning system can be increased, as shown in the first case in Fig. 1, because there is a first stop

for about 0.2 second with a high static error. Furthermore the second case in Fig. 1 illustrates a case where the phenomenon occurs even if the static error is null at the first stop, this could be damaging for the environment of the system (insertion, filling or printing tasks starting as soon as the desired position is reached). It is important to note that in Fig. 1 the two 'sticking and restarting phenomenon' have been amplified by tuning, in a non optimal way, the control parameters in order to highlight this occurrence. These two experimental tests were obtained with the test bench described in section 2.

Experiments have shown [1] that the occurrence of the restarting phenomenon is not systematic and that the instant at which it occurs is not repeatable. Up to now this undesirable effect is not well known and consequently non-predictable.

1.2 Literature review

There is no industrial or scientific research works in the literature presenting a solution that can be generalized in every fluid power process to eliminate this phenomenon. Only some specific empirical solutions have been tested in specific contexts [2 -12] to reduce the possibility of the occurrence of the 'sticking and restarting phenomenon'. There are two kinds: the first consists of technologic improvements by developing specific valves [2], the second consists in the use of specific control laws to reduce the effect of friction in electropneumatic applications by using, for example, control laws with velocity or acceleration tracking trajectories [11].

Concerning the explanation of the 'sticking and restarting phenomenon', the literature is inadequate. This paper presents and generalizes the study of this phenomenon following on from the two first works obtained respectively with simulated results [13] and experimental results [14].

1.3 Objectives of this paper

In mechanics, similar problems due to the presence of friction forces occur, giving the 'stick-slip phenomenon'. In all technologies for positioning systems it is well known that the use of an integral action in the control law can lead to a similar phenomenon. However it will be shown in this paper that in electropneumatic systems and more generally in fluid power systems, the reason for the phenomenon called 'sticking and restarting phenomenon' is fundamentally different from these two phenomena. The particularity of the fluid power positioning systems concerns the fact that both cylinder chamber pressures can evolve even if the moving part of the process has stopped in a specific position and even if the control input is constant. So this phenomenon is not only due to friction forces (like mechanical stick-slip) or to the evolution of the control law

(due to a static error combined with an integral action) but in this case there is another factor which is the pressure evolution. It will be shown that a restarting occurrence is then possible even if the desired position has been obtained (as shown in the second case of Fig. 1).

In open loop pneumatic positioning systems, there is a natural free integrator in the system from the velocity to the position state variables but this disappears when the system is in closed-loop. Furthermore, since this integrator is not placed in an upstream position with regard to the friction forces considered as disturbances, it does not act as if there was an integrator in the control law. Moreover in the literature [15] and in industrial processes (GAS, Asco Joucomatic, Norgren Company, Festo, Parker Hannifin) no integral action is used in control laws, probably to reduce the risk of the 'sticking and restarting phenomenon' occurrence. This precaution, however, is not sufficient in some cases.

The aim followed here is to explain clearly all the possibilities that lead to the 'sticking and restarting occurrence'. This is carried out from experimental results obtained with a double acting positioning system which are analyzed in order to understand the origin of this phenomenon. This contribution constitutes a first step before finding solutions to eliminate these undesirable occurrences.

In the following section, the electropneumatic system under consideration is described and modeled to help the understanding of the phenomenon. Throughout this paper the structure of the control law is considered to be a state feedback using the phase variables (position, velocity and acceleration) and no integral action. This structure of the control law, which corresponds to a partial state feedback, is classically used in fluid power control [15, 16].

The novelty of this study concerns the theoretical explanations of the 'sticking and restarting phenomenon' based on a mathematical model and experimental results. So in the third section, some mathematical definitions about equilibrium sets are recalled. The 'sticking and restarting phenomenon' is then analyzed in section 4 from an experimental result using a specific pressure force plane in order to show the studied phenomenon more easily. In section 5, a procedure for predicting the undesirable effect is given and a necessary and sufficient condition of sticking and restarting occurrence is deduced. Simulated and experimental results are then compared to validate the procedure. Finally the extension of the validity of the obtained results to other control laws or other technological fields is discussed.

2 Description and modeling of the electropneumatic positioning system considered

2.1 Description of the double acting actuator

The electropneumatic system considered is a double acting actuator. The air mass flow rates entering the two chambers are modulated by two three-way servo-distributors controlled by means of a micro-controller with two electrical inputs of opposite signs. This is described in Fig. 2. It moves a load carriage of mass M horizontally. The cylinder has a stroke of 500 millimeters and is very unsymmetric since it has an internal diameter of 32 millimeters with a simple rod of 20 millimeters diameter. The position sensor is a potentiometer. Velocity is obtained by analog derivation from the position signal and a numerical derivation of the velocity signal gives the acceleration information used by the control law. A pressure sensor is implemented in each chamber and used for analyzing the 'sticking and restarting phenomenon'.

2.2 Modeling of the system

The model presented here is used to help understand the 'sticking and restarting phenomenon'.

2.2.1 Assumptions concerning the pneumatic model

The classical assumptions [17, 18] used to obtain the model of the pneumatic part of this kind of electropneumatic system are the following:

- The supply pressure and the exhaust pressure are constant pressures,
- The air is a perfect gas and its kinetic energy is negligible in both chambers,
- The pressure and the temperature are homogeneous in each of the two chambers,
- The thermodynamic evolution of the air in the cylinder chambers is considered as polytropic and characterized by a coefficient *k*. This allows the number of state variables to be reduced.
- The temperature variations are assumed to be negligible with regards to the mean temperature, so the temperature is considered as constant and noted *T*.
- There is no mass flow leakage between the two cylinder chambers and outside the actuator.
- Using the theory of multi-time-scale systems, the dynamics of the servo-distributor can be neglected.
- The two three-way servo-distributors are identical and their electrical variable inputs are of inverse signs :

$$u_N = -u_P = -u \tag{1}$$

2.2.2 Non linear state model of the system

The non-linear state model of the electropneumatic system under consideration is 4th order and is given by the system of equations (Eq. (2)) using position, velocity and the two pressures as state variables.

$$\begin{cases} \dfrac{dp_P}{dt} = \dfrac{krT}{V_P(y)}\left[q_m(u, p_P) - \dfrac{S_P}{rT} p_P v \right] \\ \dfrac{dp_N}{dt} = \dfrac{krT}{V_N(y)}\left[q_m(-u, p_N) + \dfrac{S_N}{rT} p_N v \right] \\ \dfrac{dv}{dt} = \dfrac{1}{M}\left[S_P p_P - S_N p_N - F_f(v) - S_r p_E \right] \\ \dfrac{dy}{dt} = v \end{cases} \tag{2}$$

The two first equations concern the pneumatic part of the system. They can be obtained using the state equation of perfect gases, the mass conservation law and the polytropic law under the assumptions given above.

The two last equations describe the mechanical part. They are obtained using the fundamental mechanical equation applied to the moving part. The term $F_f(v)$ represents all the friction forces (dry and viscous) which act on the moving part.

The corresponding block diagram of Fig. 3 shows the parallel structure of the pressure dynamics. It will be shown in section 4 that the 'sticking and restarting phenomenon' can be due to the combination of this parallel structure and of the existence of dry friction forces.

The next section focuses on the friction model required to represent the friction forces acting on the moving part of the system and especially the dry friction forces which have a predominant role in the phenomenon studied.

2.2.3 Friction model

Here the aim is not to develop a sophisticated approach for friction modeling. In fact in this domain the literature is considerable [19-22]. Here only a basic friction model is necessary to achieve the aim of this paper. This elementary model has been proposed by Karnopp [23] and only stiction, Coulomb and viscous frictions

have been defined. Modeling static friction is the most difficult phase, it concerns very low velocities when the seal is stuck to the cylinder wall due to a static stiction force noted F_S. Stribeck [24] observed an exponential decrease of friction when the velocity was small and increasing. During this stage the piston moves along the cylinder wall, the seal loses its shape. This decrease in friction can reach 25% of the static stiction friction and tends towards Coulomb friction (noted F_C).

Measurements of friction forces useful to understand the 'sticking and restarting phenomenon' are shown in Fig. 4 and 5. They have been carried out using the test bench described in Fig. 2. The experimental conditions concern small displacements around the central piston position obtained with a graphically triangular shape for the desired position. These two figures show the evolution of the estimated global friction force depending on the velocity. This force is calculated at each sample time using the measured variables according to Eq. (3).

$$F_f(v) = S_P p_P - S_N p_N - S_r p_E - M \times a \tag{3}$$

In Fig. 4 the tests show a good repeatability since the experimental conditions have not varied. The model is not symmetrical. So the friction force is noted F^+ if velocity is positive and F^- in the other case.

Other tests have been carried out in other cylinder positions with different displacement amplitudes, as shown in Fig. 5 for two different position cycles. In electropneumatic actuators, the track surface quality (relating to the piston position), seal wear, working conditions (temperature, pressure, quality of air) are all parameters and variables which influence the friction values. This explains the different stiction and Coulomb friction values obtained in Fig. 5. So concerning fluid power actuators and especially pneumatic ones it is impractical to obtain valid numerical values of friction for a large domain of use. This implies that the precise analysis or the precise simulation of measured positioning results require necessarily the same working conditions for friction force identification as will be shown in sections 4 and 5.

2.3 Control law

This system is controlled by classical state feedback using the phase variables: position, velocity and acceleration (Eq. (4)). This control law presents the advantage of requiring only one sensor: the potentiometer. The velocity and acceleration are deduced from this position signal.

$$u = K_y \times \left(y^d - y\right) - K_v \times v - K_a \times a + u_0 \tag{4}$$

This constitutes a partial state feedback according to the model (Eq. (2)) and this control law does not use any integral action.

3 Some definitions of equilibrium sets

Before analyzing experimental results presenting the 'sticking and restarting phenomenon', it is necessary to recall some definitions about the different kinds of equilibrium sets.

3.1 Complete equilibrium set

3.1.1 Definition

Considering a controlled system $d\underline{x}/dt = f(\underline{x},u)$ where $\underline{x} \in \Re^n$ and $u \in \Re$, the complete equilibrium set is given by the following equation:

$$E = \left\{ \left(\underline{x}^e, u^e \right) \in \Re^n \times \Re \,/\, f\left(\underline{x}^e, u^e \right) = 0 \right\} \tag{5}$$

This means that every state variable has reached its equilibrium value.

3.1.2 Case of the electropneumatic positioning system

3.1.2.1 Description of the complete equilibrium set

According to the model (Eq. (2)) of the electropneumatic system, for a given equilibrium position y^e, the complete equilibrium set is defined by the following system of equations with the three unknown variables u^e, p_P^e and p_N^e :

$$\begin{cases} q_m\left(u^e, p_P^e\right) = 0 \\ q_m\left(-u^e, p_N^e\right) = 0 \\ S_P p_P^e - S_N p_N^e - F_f\left(v^e\right) - S_r p_E = 0 \\ v^e = 0 \end{cases} \tag{6}$$

Let us note that the complete equilibrium corresponds to the equilibrium of the mechanical part (2 last relations of Eq. (6)) which means the complete stop of the moving part of the positioning system, and to the equilibrium of the pneumatic part too (2 first relations of Eq. (6)) which represents that the two pressures do not evolve any more.

From the two first equations of (Eq. (6)), the mass flow rate entering the two cylinder chambers is equal to zero at the equilibrium state, which is obvious since there is no mass flow leakage in the cylinder. This means that the two points of coordinates (u^e, p_P^e) and $(-u^e, p_N^e)$ are derived from the static pressure gain characteristic of

the three-way servo-distributor obtained for a null mass flow rate. The experimental pressure gain characteristic of the servo-distributors used is given in Fig. 6.

From this curve, with the assumption of identical servo-distributors, the corresponding pressure force gain characteristic ($F = S_P p_P - S_N p_N$) can be built for the system composed of the two servo-distributors and the cylinder as shown in Fig. 6. It shows the evolution of the output pressure as a function of the electrical input when the output port is physically closes.

3.1.2.2 Determination of the equilibrium control input value in the case of negligible dry friction forces

To determine the equilibrium value of the electrical input u^e, let's consider in a first step, that the dry friction force is negligible at equilibrium. In these conditions, the third equation of system (Eq. (6)) leads to:

$$S_P p_P^e - S_N p_N^e = S_r p_E \tag{7}$$

which means that at equilibrium, the chamber pressures are such that the pressure force on the piston is equal to the resisting force only due in this study to the atmospheric pressure on the rod. Equation (7) means that the electrical input variable to the servo-distributors at the steady state u^e, can be found on the force characteristic from the knowledge of the resisting force ($S_r p_E$) (see Fig. 6). In the studied case, its value is different from zero due to the high non symmetric areas of the cylinder used. This value is used in the control law ($u_0 = u^e$) in order to guarantee a steady state position error equal to zero in the case of no dry friction force.

3.1.2.3 Determination of the equilibrium pressure values

According to the comments of section 3.1.2.1, the equilibrium pressure values p_P^e and p_N^e are then deduced from the pressure gain characteristic for this electrical input value u^e as shown in Fig. 6 (for more details see [14]). It is important to note that the pressure gain characteristic of the servo-distributors is of very great importance in determining the two pressure equilibrium values since for a given electrical input at the steady state u^e , the equilibrium values of the two pressures depend only on it and not on the cylinder characteristics.

The assumption of negligible dry friction was a working hypothesis for showing the graphical method of determining the equilibrium values of the state variables of the system pneumatic part more easily. With the presence of non-negligible dry friction forces the determination of the equilibrium set is more complex. It is then necessary to introduce firstly the notion of partial equilibrium defined in section 3.2, and secondly a set of

couples (u^e, p_P^e) and $(-u^e, p_N^e)$ for which the equilibrium is complete ('complete equilibrium line' described in section 4.1).

3.2 Partial equilibrium sets

3.2.1 Definition

As opposed to the complete equilibrium set E where every state variables are equal to their equilibrium values, it is possible to define partial equilibrium sets E^*. In this case, only some variables of the system state vector are at their equilibrium values (their time derivative is equal to zero):

$$\mathrm{E}^* = \left\{ \left(\underline{x}^{*e}, u^{*e} \right) \in \Re^{n^*} \times \Re \,/\, f\left(\underline{x}^{*e}, u^{*e} \right) = 0 \right\} \quad \text{with} \quad n^* < n \tag{8}$$

3.2.2 Description of the "mechanical equilibrium"

Among all physically possible cases for the electropneumatic system considered, one kind of partial equilibrium set is interesting to note. It concerns the equilibrium of the mechanical part only: the system is stopped but the pressure in one or two chambers evolves. This defines the "*mechanical equilibrium*".

The following system of equations (Eq. (9)) deduced from the non linear model (Eq. (2)) and, using the variables with the superscript '**e*' for those being at the 'mechanical equilibrium', describes this partial equilibrium:

$$\begin{cases} \begin{cases} \dfrac{dp_P(t)}{dt} = \dfrac{krT}{V_P\left(y^{*e}\right)} q_m\left(u^{*e}, p_P(t)\right) \\ \dfrac{dp_N(t)}{dt} = \dfrac{krT}{V_N\left(y^{*e}\right)} q_m\left(-u^{*e}, p_N(t)\right) \end{cases} & \text{pneumatic part} \\ \begin{cases} \dfrac{dv^{*e}}{dt} = \dfrac{1}{M}\left[S_P p_P(t) - S_N p_N(t) - F_f\left(v^{*e}\right) - S_r p_E\right] = 0 \\ \dfrac{dy^{*e}}{dt} = v^{*e} = 0 \end{cases} & \text{mechanical part} \end{cases} \tag{9}$$

3.2.3 Stop conditions of the moving part

In the general case of presence of dry friction forces, considering the third equation of (Eq. (2)) and according to the considered friction model (section 2), the system stops if, when the velocity becomes zero, the sum of the pressure forces applied to the moving part is lower than the Coulomb dry friction. Here the forces are the pressure force (due to chamber pressures) and the one due to the atmospheric pressure on the rod ($S_r p_E$). Let

us note t^{stop}, the instant of stopping and thus $p_P^{stop} = p_P\left(t^{stop}\right)$ and $p_N^{stop} = p_N\left(t^{stop}\right)$. This leads to Eq. (10) which defines a set of possible couples of pressures (p_P^{stop} , p_N^{stop}) at this instant:

$$F_C^- < S_P p_P^{stop} - S_N p_N^{stop} - S_r p_E < F_C^+ \tag{10}$$

From this time and onward while the moving part is stopped, according to the chosen control law (Eq. (4)), the control input of the system depends only on the position error and thus stays constant and equal to:

$$u^{*e} = K_y \times \left(y^d - y^{*e}\right) + u_0 \tag{11}$$

In most cases however, at this moment the pressures values p_P^{stop} and p_N^{stop} are not equal to their equilibrium values $p_P{}^e$ and $p_N{}^e$ determined from the pressure gain characteristic as shown in Fig. 6 for respectively u^{*e} and $-u^{*e}$ (section 3.1.2.3). The two pressures go on changing, their evolution towards p_P^e and p_N^e being given by the two first non linear equations of system (Eq. (9)).

This means that as soon as the moving part stops, the electropneumatic system is only in a partial equilibrium corresponding to the mechanical equilibrium.

4 Analysis of the restarting phenomenon

4.1 Pressures time evolution representation in an adequate plane

As soon as the mechanical part stops and during all the mechanical equilibrium, the model of the electropneumatic positioning system is the one described by (Eq. (9)) and consists of only two state variables : the two chamber pressures.

In order to better understand the restarting phenomenon and to make clear the difference between the complete equilibrium and the partial one, it is interesting to plot the time evolution of these chamber pressures in a plane showing the different working areas depending on the dry friction forces and on the pressure gain characteristic of the servo-distributors.

This plane can be directly related to the pressure plane (already introduced in a simulation context [13]) or a pressure force plane. Here we use a plane whose axes are $S_P p_P$ and $S_N p_N + S_r p_E$ to show the pressure force evolution (deduced from the pressure evolution). Different curves can be drawn (Fig. 7) on this plane:

- Firstly, the points deduced from the pressure gain characteristic of the servo-distributors (Fig. 6) corresponding to null mass flow rates and graduated by *u* values: each pair of pressure forces is obtained for a value *u* of the power modulators electrical input. During the 'mechanical equilibrium', the curve representing the time evolution of the two pressures evolves towards one of these particular points of the plane (the one corresponding to the control input u^{*e}).

- Secondly, two dotted lines showing the limits of the Coulomb dry friction. Their equations in the plane are deduced from Eq. (10) which gives the limit values of the force $S_N p_N + S_r p_E$ for which the system does not move as a function of the pressure force on the P side of the piston $S_P p_P$. These two lines define an area called 'stop area':

$$S_P p_P - F_C^+ \leq S_N p_N + S_r p_E \leq S_P p_P - F_C^- \tag{12}$$

Equation (12) means that as soon as the pressure force trajectory of the system enters into this area with a very low velocity, the moving part stops. The corresponding point of the plane is ($S_P p_P^{stop}, S_N p_N^{stop} + S_r p_E$).

- Thirdly, two straight lines showing the limits of the stiction friction whose equations are similar :

$$S_P p_P - F_S^+ \leq S_N p_N + S_r p_E \leq S_P p_P - F_S^- \tag{13}$$

The area (Eq. (13)) defined by these two last lines defines the pressure force relationship at zero velocity, when the system cannot move. It is called the 'no restarting area'. The pressure forces trajectory must evolve outside this area to make the system move.

It is interesting to note in Fig. 7 that the slope of these four straight lines is equal to one and that their ordinate at the origin gives the value of the corresponding dry friction force with the opposite sign.

According to the results of section 3.1.2, extended to the case of the presence of dry friction forces, when the electropneumatic system is in a complete steady state the point corresponding to the equilibrium pressures is located in the plane of Fig. 7 on the curve deduced from the pressure gain characteristic for a null mass flow rate (condition given by the two first equations in Eq. (6)) but only in the 'no restarting area' (condition given by Eq. (13)). This particular piece of curve is noted 'complete equilibrium line' and shown in Fig. 7 by a continuous line.

During mechanical equilibrium, the pressures evolve towards their equilibrium values p_P^e and p_N^e deduced from the pressure gain at null mass flow rate for the control input u^{*e}. It is then possible to deduce these two results:

⇨ If the point of co-ordinates $(S_P p_P^e, S_N p_N^e + S_r p_E)$ is outside the 'complete equilibrium line' (this means on the dotted part of the curve described in Fig. 7), the pressure trajectory during the partial equilibrium (mechanical equilibrium) will obviously evolve outside the 'no restarting' area and thus the system will move. It is then systematic in this case.

⇨ In the other case, the mechanical equilibrium leads to a complete equilibrium only if the time evolution of the two pressures lead to a curve totally included in the 'no restarting area'. The force due to the pressures in each chamber does not induce a force greater than the stiction force and so the cylinder does not move. It is not always the case and the 'sticking and restarting phenomenon' can occur. This occurrence is mainly due to the parallel structure of the system corresponding to the two pressure dynamics shown in Fig. 3, and can appear even if the steady state position error is zero (as shown on Fig. 1).

4.2 Experiment analysis

In order to analyze the 'sticking and restarting phenomenon', this section uses experimental results shown in Fig. 8. This consists of an example of a step response for the positioning system described in section 2. The desired position is a negative displacement of 50 millimeters near the positive end of stroke of the cylinder (see Fig. 2). There is an initial stop (at time t_2), then the moving part moves again (between instants t_3 and t_4) with a displacement magnitude of 0.74 millimeters (Fig. 8a). This is an occurrence of the 'sticking and restarting phenomenon' with a sticking phase that lasts 4 seconds. Figure 8b illustrates what happens during this sticking stage: the two chamber pressures go on evolving whereas the control law stays constant. It is interesting to note that the chamber 'P' pressure evolves with a magnitude and duration much larger than the chamber 'N' pressure.

In what follows, the evolution of the electropneumatic system considered (Fig. 2) will be studied in detail during five time intervals corresponding to the five different phases (movement, partial or complete equilibrium), using the proposed pressure force plane of Fig. 7.

Since the experimental test of Fig. 8 shows a restarting phenomenon in the opposite direction to the previous displacement, it is possible to determine the four dry friction forces required by the model in Fig. 4. This can be carried out by building the total pressure force time evolution according to Eq. (14) calculated at each sample time and shown in Fig. 9.

$$F(t) = S_P p_P(t) - S_N p_N(t) - S_r p_E \tag{14}$$

By identification, the force values are determined according to the Eq. (15).

$$\begin{cases} \text{at start time} & t = t_1 \quad F(t_1) = F_f = F_S^- \\ \text{at the first stop} & t = t_2 \quad F(t_2) = F_f = F_C^- \\ \text{at restarting time} & t = t_3 \quad F(t_3) = F_f = F_S^+ \\ \text{at the second stop} & t = t_4 \quad F(t_4) = F_f = F_C^+ \end{cases} \tag{15}$$

4.2.1 Analysis before the first movement: from t=t_i to t= t_1

This phase between t_i and t_1 is very short (87 ms), and is not visible in Fig. 8 and 9 but the pressure force plane representation illustrates it more precisely in Fig. 10.

At initial time called t_i, the point with coordinates $\left(S_P p_P(t_i), S_N p_N(t_i) + S_r p_E\right)$ with y^e=0.2195m is included in the 'stop area'. It corresponds to a complete equilibrium of the system.

The desired position is a step from y^d=0.220 m to y^d=0.170 m. The cylinder does not move immediately even if the control input is very high due to a high position error because of dry friction forces. However the pressures evolve quickly in each chamber (mainly the pressure in chamber P) as shown in Fig. 10 by the pressure force trajectory between its initial value in the 'stop area' and its intersection with the straight line corresponding to $F_f = F_S^-$ for $t = t_1$. At this time, the pressure force curve goes out of the 'no restarting area' which means that the pressures create a force greater than the stiction friction (F_S^-), so the system moves.

4.2.2 Analysis before the first stop: from t=t_1 to t= t_2

This phase corresponds to the main dynamic stage. It is interesting to note in Fig. 10 that just before the stop, the pressure force trajectory evolves near the straight line defined by the Coulomb friction value F_C^-. These oscillations correspond in fact to microscopic 'sticking and restarting phenomena'. However due to the position sensor precision, this observation is not visible on the position signal. At time t = t_2 corresponding to the first stop, the curve is entering the 'stop area', the static error is large and is 0.87 mm.

4.2.3 Analysis during the first stop: from t=t_2 to t= t_3

From the time t = t_2 to t = t_3, the equilibrium set is partial and it corresponds to the 'mechanical equilibrium' defined in section 3.2.2. During all this phase, as the moving part is stopped, the control signal is constant and

noted u^{*e}, however the pressure in each chamber evolves towards its value on the pressure gain curve corresponding to this control value u^{*e}. In the case studied, this point is outside the 'complete equilibrium line' defined above and shown in Fig. 7. Figure 11 shows that at $t = t_3$, the corresponding pressure force curve goes outside the 'no restarting area', indicating that the pressure force becomes greater than the stiction force ($F(t) \geq F_s^+$) and then the positioning system moves again. As the control signal is constant during all this phase, the restarting phenomenon is not due, in this case, to an integral action in the control law.

It is clear in Fig. 8 and 11 that the pneumatic equilibrium is obtained in chamber N before chamber P. This is due to the fact that the two pressure dynamics are very different, mainly because the volume of chamber P is much greater than the volume of chamber N (piston position near the positive stroke end). Using the linearized model for the pressure dynamics, it can be found that the time constant of the pressure p_P dynamics is about eight times higher in this case than the time constant of the pressure p_N [25].

As a consequence, the restarting occurrence is more frequent when the cylinders are very asymmetrical (case of simple rod with large diameter piston) and when the desired position is near the end of the stroke.

4.2.4 Analysis before the second stop: from $t=t_3$ to $t= t_4$

Once the system moves again, a new control signal value is calculated at each sample time, so the total force $F(t)$ converges quickly to F_C^+ (Fig. 11). The new static error is less significant at 0.13 mm

4.2.5 Analysis from $t=t_4$ to $t=t_f$:

During this entire interval the control signal is constant. The two pressures evolve towards their equilibrium values without going out of the 'no restarting area'. The pneumatic equilibrium is obtained, which means that the partial mechanical equilibrium set converges to a complete equilibrium set (see Fig. 11).

The table 1 summarizes and quantifies the different stages obtained during the positioning step response in order to complement Fig. 10 and 11.

5 Theoretical conclusions

The analysis of the experimental results carried out above enables us to establish two mathematical results presented in this section:

- the first one concerns a necessary and sufficient condition for which the electropneumatic system does not restart after the first stop,
- the second one gives an approximation of the time at which the system will restart if the condition above is not verified.

5.1 Necessary and sufficient condition to not have the occurrence of the restarting phenomenon

Let us consider a double sided electropneumatic actuator (having no flow leakage) moving a load using two identical 3/2 way servo-distributors controlled by opposite signs. If the control signal 7is synthesized in such a manner as it remains constant as soon as the moving part stops at $t=t^{stop}$ (noted u^{*e} during all the mechanical partial equilibrium), the **necessary and sufficient condition** to avoid a restarting stage, is the following**:**

$$\forall t \geq t^{stop}, \quad F_S^- < F(t) < F_S^+ \tag{16}$$

where $F(t)$ can be approximated by Eq. (17):

$$F(t) = S_P\left(p_P^{stop} - p_P^e\right)e^{-\frac{t-t^{stop}}{\tau_P^{stop}}} - S_N\left(p_N^{stop} - p_N^e\right)e^{-\frac{t-t^{stop}}{\tau_N^{stop}}} + S_P p_P^e - S_N p_N^e - S_r p_E \tag{17}$$

F_S^- and F_S^+ are the stiction force values at the stop position y^{*e},

p_P^{stop} and p_N^{stop} are the chamber pressure values at the stop time $t = t^{stop}$

p_P^e and p_N^e are the chamber equilibrium pressure values deduced from the servodistributor pressure gain characteristic at null mass flow rate for the u^{*e} control value (Fig. 6).

τ_P^{stop} and τ_N^{stop} are the chamber pressure time constants corresponding to the linearized tangent pressure model around the stop conditions assumed to be valid during all the mechanical partial equilibrium.

5.2 Proof

It has been shown in the previous section that as soon as the actuator stops at the instant noted t^{stop}, the whole electropneumatic system is in a partial equilibrium corresponding to the 'mechanical equilibrium'. The state variables belonging to the partial equilibrium set, as defined by (Eq. 8), are noted with the superscript '*e' and they stay equal to their value at the stop time:

$$\begin{cases} y^{*e} = y\left(t^{stop}\right) \\ v^{*e} = v\left(t^{stop}\right) = 0 \\ u^{*e} = u\left(t^{stop}\right) = K_y\left(y^d - y\left(t^{stop}\right)\right) = K_y\left(y^d - y^{*e}\right) \end{cases} \tag{18}$$

According to Eq. (9), after this stop and while the moving part does not move, this partial equilibrium is described by the algebraic-differential system on Eq. (19):

$$\begin{cases} \dfrac{dp_P(t)}{dt} = \dfrac{krT}{V_P\left(y^{*e}\right)} q_{m\,P}\left(u^{*e}, p_P(t)\right) \\ \dfrac{dp_N(t)}{dt} = \dfrac{krT}{V_N\left(y^{*e}\right)} q_{m\,N}\left(-u^{*e}, p_N(t)\right) \\ F_f(t) = S_P p_P(t) - S_N p_N(t) - S_r p_E \\ v^{*e} = 0 \end{cases} \tag{19}$$

with:

$$F_C^- \le F_f\left(t^{stop}\right) \le F_C^+ \qquad \text{Stop area} \tag{20}$$

$$F_S^- \le F_f\left(t^{stop} < t \le t^{move}\right) \le F_S^+ \qquad \text{No restarting area} \tag{21}$$

Equation (20) recalls that the system stops if, for a velocity near zero, the sum of the forces applied to the moving part becomes less than the Coulomb friction force, that is to say that the force pressure curve in the pressure plane defined in section 4 is inside the 'stop area'.

If the moving part restarts after the stop at the instant noted t^{move}, this means that the force pressure curve goes outside the 'no restarting area'. So during the entire mechanical equilibrium phase, the curve stays inside this area as described by Eq. (21).

As shown by the experiments analyzed in section 4, the restarting occurs or does not occur depending on the pressure force evolution. In order to study this evolution more easily, the two first non linear equations of Eq. (19) governing the two pressure evolutions are linearized around the stop conditions [25]. The linear model (Eq. (22)) approximating the pressure evolutions is as follows.

$$\begin{cases} \dfrac{d\delta p_P\left(t - t^{stop}\right)}{dt} = -\dfrac{1}{\tau_p^{stop}} \delta p_P\left(t - t^{stop}\right) + \dfrac{krT}{V_P(y^{*e})} q_m\left(u^{*e}, p_P^{stop}\right) \\ \dfrac{d\delta p_N\left(t - t^{stop}\right)}{dt} = -\dfrac{1}{\tau_N^{stop}} \delta p_N\left(t - t^{stop}\right) + \dfrac{krT}{V_N(y^{*e})} q_m\left(-u^{*e}, p_N^{stop}\right) \end{cases} \tag{22}$$

with the following notations useful to define the two pressure time constants τ_P^{stop} and τ_N^{stop} :

$$\begin{cases} C_{p_P}^{stop} = - \left. \dfrac{dq_{m\,P}\left(u^{*e}, p_P\right)}{dp_P} \right|_{\left(p_P^{stop}\right)} \\ \delta p_P\left(t - t^{stop}\right) = p_P\left(t - t^{stop}\right) - p_P^{stop} \\ \tau_p^{stop} = \dfrac{V(y^{*e})}{krTC_{p_P}^{stop}} \end{cases} \quad \text{and} \quad \begin{cases} C_{p_N}^{stop} = - \left. \dfrac{dq_{m\,N}\left(-u^{*e}, p_N\right)}{dp_N} \right|_{\left(p_N^{stop}\right)} \\ \delta p_N\left(t - t^{stop}\right) = p_N\left(t - t^{stop}\right) - p_N^{stop} \\ \tau_N^{stop} = \dfrac{V(y^{*e})}{krTC_{p_N}^{stop}} \end{cases} \tag{23}$$

Servo-distributors of good quality usually exhibit a pressure gain characteristic at null mass flow rate with an important slope (see Fig. 6). This means that the u^{*e} value is in the central part of this curve. Furthermore the steady state mass flow rate characteristics versus pressure are nearly linear for the control values corresponding to the central part of this slope (± 10% u_{MAX}) (see Fig. 12). This remark justifies the local linearization carried out and the validity of the corresponding model (Eq. (22)).

The solutions of the two linear differential relations (Eq. (22)) are:

$$\begin{cases} p_P\left(t - t^{stop}\right) = \left(p_P^{stop} - p_P^e\right) e^{-\frac{t - t^{stop}}{\tau_P^{stop}}} + p_P^e \\ p_N\left(t - t^{stop}\right) = \left(p_N^{stop} - p_N^e\right) e^{-\frac{t - t^{stop}}{\tau_N^{stop}}} + p_N^e \end{cases} \tag{24}$$

The time evolution of the force *F* that is opposed to the dry friction during the partial mechanical equilibrium can then be approximated by Eq. (17).

According to Eq. (21), if after the stop time, the force *F(t)* stays inside the $\left[F_S^-, F_S^+\right]$ domain corresponding to the 'no restarting area', then the partial mechanical equilibrium leads to a complete equilibrium defined by the system (Eq. (6)). The pressures reach their equilibrium values p_P^e and p_N^e corresponding to the control value $u^e = u^{*e}$. This leads to the no restarting condition proposed in Eq. (16).

5.3 Estimation of the restarting time if the 'non restarting condition' is not verified.

If there is an instant at which the global pressure force *F(t)* is no longer included in the $\left[F_S^-, F_S^+\right]$ domain, the 'non restarting condition' (Eq. (16)) is no longer in effect: the partial mechanical equilibrium does not lead to a complete equilibrium of the system. The cylinder moves again and a new control signal is calculated. At the

instant at which the load restarts, the global pressure force is equal to the stiction force. Using the force approximation of (Eq. (17)), an estimate of this instant thus verifies one of the two equations of (Eq. (25)). It is noted t^{move+} or t^{move-} according to the stiction values (respectively F_S^+ or F_S^-) the force F is equal to.

$$\begin{cases} S_P\left(p_P^{stop}-p_P^e\right)e^{-\frac{t^{move+}-t^{stop}}{\tau_P^{stop}}}-S_N\left(p_N^{stop}-p_N^{\mathrm{e}}\right)e^{-\frac{t^{move+}-t^{stop}}{\tau_N^{stop}}}+S_P p_P^e-S_N p_N^e-S_r p_E=F_S^+ \\ S_P\left(p_P^{stop}-p_P^e\right)e^{-\frac{t^{move-}-t^{stop}}{\tau_P^{stop}}}-S_N\left(p_N^{stop}-p_N^e\right)e^{-\frac{t^{move-}-t^{stop}}{\tau_N^{stop}}}+S_P p_P^e-S_N p_N^e-S_r p_E=F_S^- \end{cases} \quad (25)$$

Equation (25) which includes the expression of the time at which the system will move again can only be solved numerically because it is of the form: $Ae^{-\alpha x}+Be^{-\beta x}=C$.

5.4 Application of the theoretical results to the example of section 3

In this section, the two previous theoretical results are illustrated in the first mechanical partial equilibrium of the example analyzed in section 4. That is from the first stop ($t=t_2$) up to the instant at which the moving part restarts ($t=t_3$). Figure 13 shows the comparisons of simulated pressures and force time evolution with the experimental ones during this mechanical partial equilibrium. The instant $t=t_2$ at which the stop occurs is taken as the time reference. The experimental force is calculated using the pressure measurements according to Eq. (14). The simulated pressures and force are respectively obtained using the approximations of Eq. (24) and Eq. (17). The equilibrium pressure values p_P^e and p_N^e are deduced from the experimental pressure gain characteristic (Fig. 6) for the experimental control input value u^{*e} corresponding to the partial equilibrium considered. Furthermore the pressure time constants are calculated from Eq. (23) using the slope of the measured mass flow rate characteristics according to the pressures (Fig. 12).

Figure 13 shows that the linearized pneumatic model (Eq. (24)) enables the global reproduction of the real evolution of pressures and force. The use of a better thermodynamic model taking into account the thermal exchanges taking place in the chambers could improve the precision of the simulation results. However it is sufficient to point out that there is an instant at which the force becomes greater than the stiction force inducing the restarting of the moving part according to Eq. (16-17).

Furthermore, using the first equation of Eq. (25), it is possible to have an estimation of the duration of the partial equilibrium set when it does not lead to complete equilibrium and so the instant of the restarting phenomenon.

Solving numerically Eq. (25) (or reading this time on the simulated curve of figure 13b), gives the result $t^{move+} - t^{stop} = 3.80$ seconds, which is very close to the experimental result t_3-t_2 of the table 1 of 3.86 seconds.

However it must be noted that this coherence between measurement and simulation has been obtained due to an accurate characterization of the flow stage of the servo-distributor, especially for the control values corresponding to the slope of the pressure gain characteristic [13]. It consists of measured data of the servo-distributor output mass flow rate values as a function of the control input values and of the output pressure values. This data must enable the precise slopes ($C_{p_P}^{stop}$ and C_{pN}^{stop}) of the two mass flow rate curves as a function of the output pressures corresponding to the control values u^{*e} and $-u^{*e}$ at the 'stop conditions' i.e. for p_p^{stop} and p_N^{stop} to be obtained.

6 Conclusions

The contribution of this paper concerns the explanation of the 'sticking and restarting phenomenon' of electropneumatic systems.

It has been shown that this phenomenon can be explained by the fact that at the first stop of the moving part, the system has not reached its complete equilibrium but only a partial one called 'mechanical equilibrium'. The system is stopped by the fact that the global pressure force becomes smaller than the Coulomb dry friction force. From this instant, the two chamber pressures go on evolving to their equilibrium values corresponding to the control input which stays constant. Even if these equilibrium values correspond to a complete equilibrium, during its evolution the global pressure force can become greater than the stiction force, inducing the restarting phenomenon. This is possible because of the parallel structure of the system which corresponds to the pressure dynamics.

It must be noticed that this parallel structure appears in electrohydraulic systems too. However the 'sticking and restarting phenomenon' is less awkward than in electropneumatics since the restarting time is shorter due to higher pressure dynamics. In fact the compressibility of oil is lower than for air which means that the quantity of hydraulic fluid required to reach equilibrium pressure is smaller than for the pneumatic one.

This analysis has led to two theoretical results: the first one concerning a necessary and sufficient condition not to have the restarting phenomenon, the second one giving an estimation of the restarting time if the condition is not in effect. These two results have been validated by the experimental result studied mainly because the

required dry friction values were identified in the same conditions and because a precise model of the servo-distributor flow stage was known. Otherwise, if these conditions are not validated, these two theoretical results can not be used in a predictive manner. However, these results could be useful to find solutions to avoid the undesirable phenomenon of restarting.

The problem of the restarting phenomenon is more and more present, because manufacturers try to reduce the friction forces with different kinds of new seals, which leads to a reduction of the 'no restarting area'. So a compromise must be found between the static error and the restarting occurrence. The solutions must be included in the control strategy as in [26-30]. It must be noticed that the results obtained in this paper are valid for every kind of control law for which the control value does not evolve during the partial mechanical equilibrium. If this is not the case, the occurrence of the restarting phenomenon is less obvious to predict. However a 'controlled' evolution of the control value during the mechanical equilibrium could be a way to try to avoid this undesirable event.

Nomenclature

a	acceleration (m/s^3)
$C_{pP/N}^{stop}$	derivation of the mass flow rate $q_{mP/N}$ according to $p_{P/N}$ around the stop state (kg/s/Pa)
e	complete equilibrium set
e^*	partial equilibrium set
F	force (N)
k	polytropic constant
K_y, K_v, K_a	position gain (V/m), velocity gain (V/m/s) and acceleration gain(V/m/s^2)
M	total load mass (kg)
n	order of the system
p	pressure (Pa)
$q_{mP/N}$	mass flow rate provided from by the servo-distributor to cylinder chamber P or N (kg/s)
r	perfect gas constant related to unit mass (J/kg/K)
$S_{P/N}$	area of the cylinder piston on the chamber P or N side (m^2)
S_r	rod area (m^2)
t	time (s)
T	temperature (K)
u	servo-distributor input voltage (V)
u_0	servo-distributor input voltage to compensate the non symmetry (V)
v	velocity (m/s)
V	volume (m^3)
$\underline{x}$	state vector
y	position (m)
δ	variation around the equilibrium set
$\tau_{P/N}$	chamber P or N pressure time constant (s)

Subscript

C	Coulomb friction
E	exhaust
f	friction
N	relative to chamber N

P	relative to chamber P
r	rod
S	stiction friction

Superscript

d	desired
e	equilibrium
+	positive direction
-	negative direction
*	relative to partial equilibrium
stop	stop of the movement

References

[1] **Brun, X., Thomasset, D., Bideaux, E.**, *"Influence of the process design on the control strategy: application in electropneumatic field"*, Control Engineering Practice, Vol 10, Issue 7, July 2002, Pages 727-735.

[2] **Harrold, D.,** "Select and Size Control Valves Properly to Save Money", available on http://www.manufacturing.net/ctl/index.asp?layout=article&articleid=CA192621, Oct 1999 Control Engineering

[3] **Armstrong-Hélouvry, B., Dupont, P., Canudas de Wit, C.** *A survey of analysis tools and compensation methods for the control of machines with friction.* Automatica, 1994, Vol. 30, p 1083-1138.

[4] **Kimura, T., Hara, S., Fujita, T., Kagawa, T.** *Feedback Linearization for Pneumatic Actuator Systems with Static Friction.* Control Eng. Practice, 1997, Vol. 5, n°10, p 1385-1394.

[5] **Tafazoli, S.** *Tracking control of an Electrohydraulic Manipulator in the presence of Friction.* IEEE Trans. on Cont. Syst. Tech., May 1998, Vol. 6, n°3, p 401-411.

[6] **Kang, M.S.** *Robust digital friction compensation*. Cont. Eng. Prac, 1998, Vol 6, n°3, p 359-367.

[7] **Tokashiki Kishimoto, L.R.,** *Dynamic Characteristics of Pneumatic Cylinder Systems*, Thèse: Sci.: Tokyo Institute of Technology, 1999, 133 p.

[8] **Suzuki, A., Tomizuka, M.,** *Design and Implementation of Digital Servo Controller for High Speed Machine Tools* Proc. AACC, Boston, 1991, p 1246-1251.

[9] **Cheng, C.C, Chen, C.Y.** *A PID approach to suppressing stick-slip in the positioning of transmission mechanisms.* Cont. Eng. Pract., 1998, Vol 6 n°4, p 359-367.

[10] **Hamiti, K., Voda-Besançon, A., Roux-Buisson, H.,** *Position Control of a Pneumatic Actuator Under the influence of Stiction.* Control Eng. Practice, 1996, Vol. 4, n°8, p 1079-1088.

[11] **Ming-Chang, S., Shy-I, T.,** *"Identification and position control of a servo pneumatic cylinder",* Control Engineering Practice, Volume 3, Issue 9 , September 1995 , Pages 1285-1290

[12] "Servo pneumatics finding its niche, bit by bit", April-May 2003, Vol 4, Number 1, p32-33, Control Engineering Europe

[13] **Sesmat, S., Scavarda, S.,** *Study of the behavior of an electropneumatic positioning system near the equilibrium state.* 1st Int. Fluid. Kolloq. in Aachen, Aachen, 17-18 Marz, 1998, vol. 2, p 321-334.

[14] **Brun, X., Sesmat, S., Scavarda, S., Thomasset**, D. *Simulation and experimental study of the partial equilibrium of an electropneumatic positioning system, cause of the 'sticking and restarting phenomenon'*, 4th Jap Hydraulics and Pneumatics Society Int. Symp. on Fluid Power, *Tokyo*, Japan, 15-17 Nov 1999, p 125-130.

[15] **Edge, K. A.**, *The control of fluid power systems - responding to the challenge.* Journal of Systems and Control Engineering, 1997, Vol 211, N°12, p. 91-110.

[16] **Richard, E., Scavarda, S.,** *Comparison between Linear and Nonlinear control of an eletropneumatic servodrive.* J. of Dynamic Systems, Measurement, and Control, June 1996, Vol. 118, p. 245-252.

[17] **Shearer, J.L.,** *Study of pneumatic processes in the continuous control of motion with compressed air.* Parts I and II. Trans. Am. Soc. Mech. Eng., 1956, Vol. 78, p. 233-249.

[18] **Mc Cloy, D.,** *Discharge characteristics of servo valve orifices.* In: The 1968 Fluid Power International conference, Olympia, Paper 6, 1968, p 43-50.

[19] **Tustin A.,** The Effect of Backlash and Speed-dependent Friction on the Stability of closed-cycle control systems. Jour. of the Institution of Electrical Engineers, Vol. 94, n°2A, 1947, pp 143-151.

[20] **Dahl, P. R.,** A Solid friction Model. TOR-158, The Aerospace Corporation, El Segundo, California, 1968, pp 3107-3118.

[21] **Armstrong-Hélouvry, B., Dupont, P., Canudas de Wit, C.,** A survey of analysis tools and compensation methods for the control of machines with friction. Automatica, 30, 1994, pp 1083-1138.

[22] **Canudas de Wit, C., Olsson, H., Aström, K.J., Lischinsky, P.,** A new model for control of systems with friction. IEEE Transactions on Automatic Control, Vol. 40, n°3, 1995, pp 419-425.

[23] **Karnopp, D.,** Computer Simulation of Stick-Slip Friction in Mechanical Dynamic Systems. Journal of Dynamic Systems, Measurement and Control, March 1985, Vol. 107, p 100-103.

[24] **Stribeck**, **R.,** *Die Wesentlichen eigenschaften der Gleit und Rollenlager – the key qualities of sliding and roller bearings*. Zeitschrift des Vereines Seutscher Ingenieure, 1902, 46(38), p. 1342-1348;46(39), p. 1432-1437

[25] **Brun, X., Belgharbi, M., Sesmat, S., Thomasset, D., Scavarda, S.,** *Control of an electropneumatic actuator, comparison between some linear and nonlinear control laws*, Journal of Systems and Control Engineering, 1999, Vol. 213, N°I5, p 387-406.
[26] **Johnson, C.T., Rolenz, R.D.,** *Experimental identification of friction and its compensation in precise position controlled mechanism.* IEEE Trans. Ind. Applic, 1992, Vol 28, N°6, p 1392-1398.
[27] **Canudas de Witt, C., Åström, K. J., Braun, K.,** *Adaptive friction compensation in dc-motor drive,* IEEE Jounal Robotics Automn, 1987, RA-3 (6), p681-685.
[28] **Ray, R., L., Ramasubramanian, A., Townsend, J.,** *Adaptive friction compensation using extended Kalman-Bucy filter friction estimation,* . Control Eng. Practice, 2001, Vol. 9, n°2, p 169-179.
[29] **Cho, S.H., Edge, K. A.,** *Adaptive sliding mode tracking control of hydraulic servosystems with unknown non-linear friction and modeling error*, Journal of Syst. and Control Eng., 2000, Vol. 214, N°I4, p 247-258.
[30] **Choi, S.H., Lee, C.O. Cho, S.H.,** *Friction compensation control of an electropneumatic servovalve by using an evolutionary algorithm*, Journal of Systems and Control Engineering, 2000, Vol. 214, N°I3, p 173-184.

Time [s]	Event	Equilibrium	Position [mm]	Static error [mm]	$F(t)$ [N]
t_i=1.000	Stop	Complete	219.52	0.48	$\in \left[F_C^-, F_C^+\right]$
t_1=1.087	Starting in negative direction	Dynamic stage	219.52	0.48	F_S^-
t_2=1.675	First stop	Partial : mechanical	169.13	0.87	F_C^-
t_3=5.536	Restarting in positive direction	Dynamic stage	169.13	0.87	F_S^+
t_4=5.816	Second stop	Partial : mechanical	170.13	0.13	F_C^+
t_f=12.000	End	Complete	170.13	0.13	$\in \left[F_C^-, F_C^+\right]$

Table 1: Characteristics of the different stages

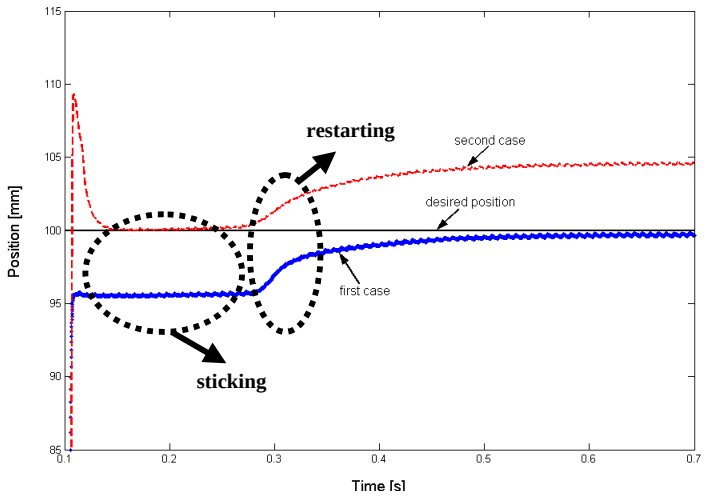

Fig. 1 Two experimental cases of the 'sticking and restarting phenomenon' in electropneumatic systems (zoom of the end of displacements)

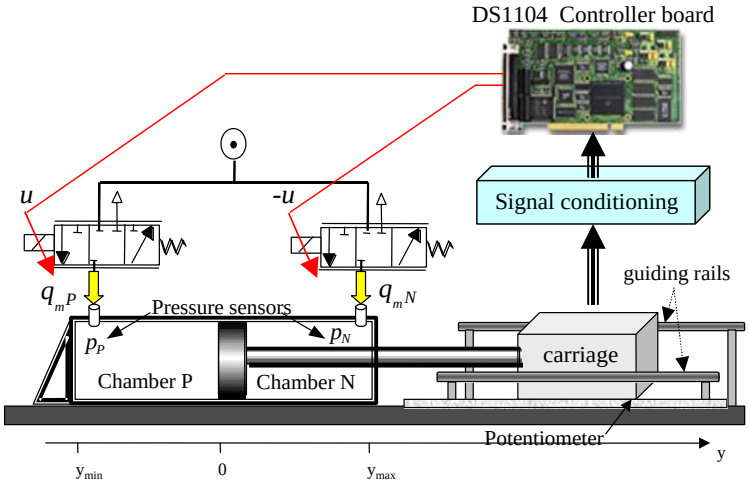

Fig. 2 The double acting electropneumatic actuator under consideration

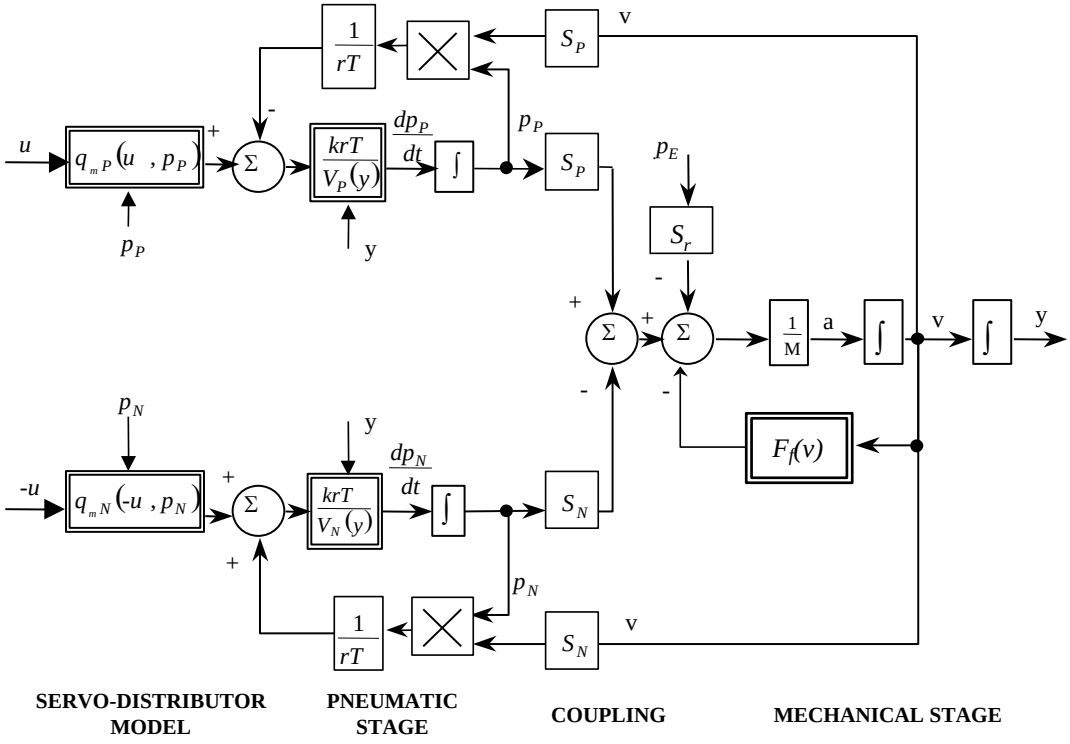

Fig 3 Non linear block diagram of the electropneumatic actuating system

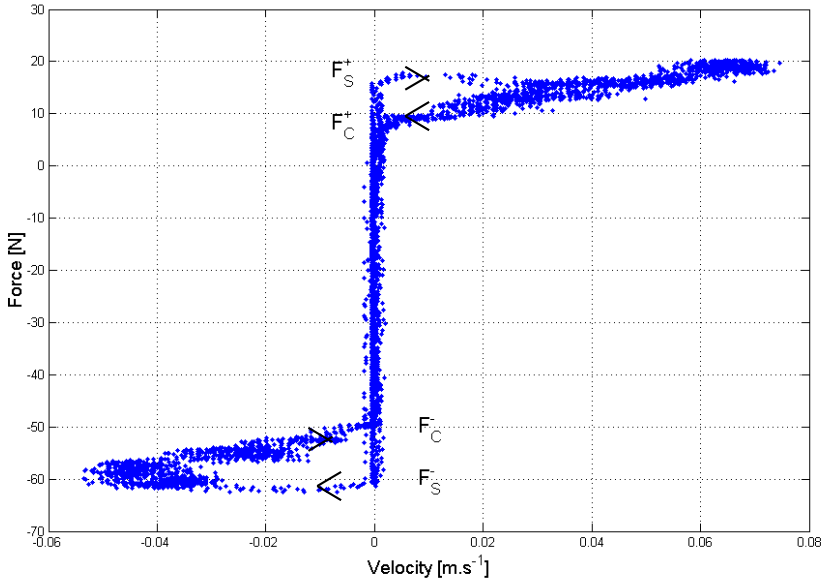

Fig 4 Experimental results showing the different friction phenomena

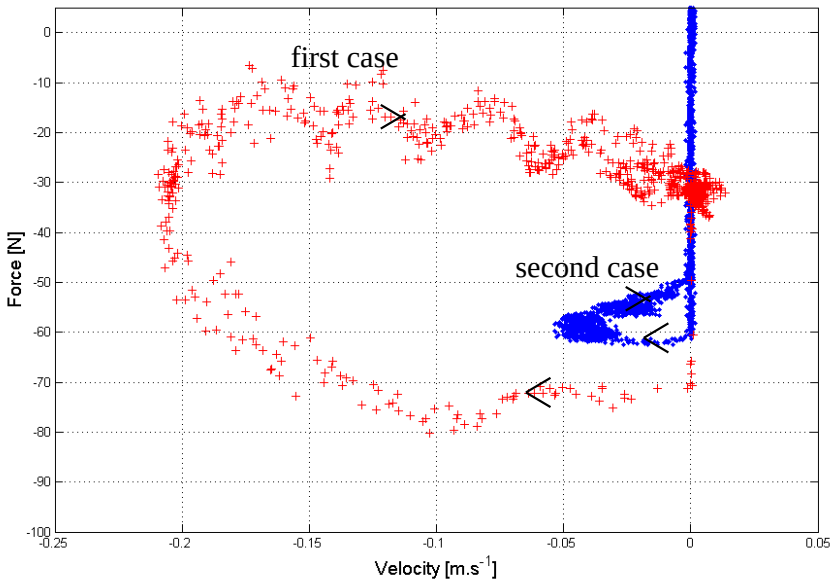

Fig 5 Friction forces for two different experimental conditions

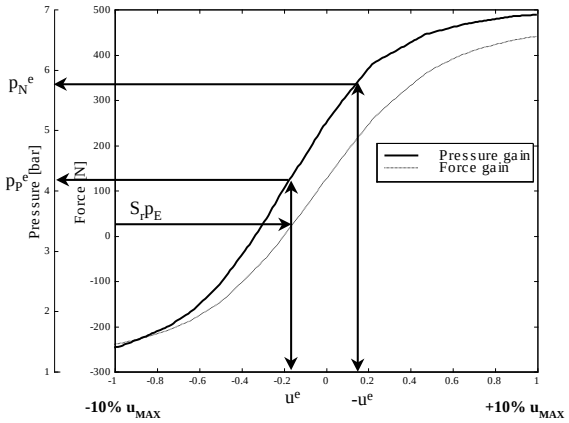

Fig 6 Graphic determination of equilibrium variables in the case of negligible dry friction.

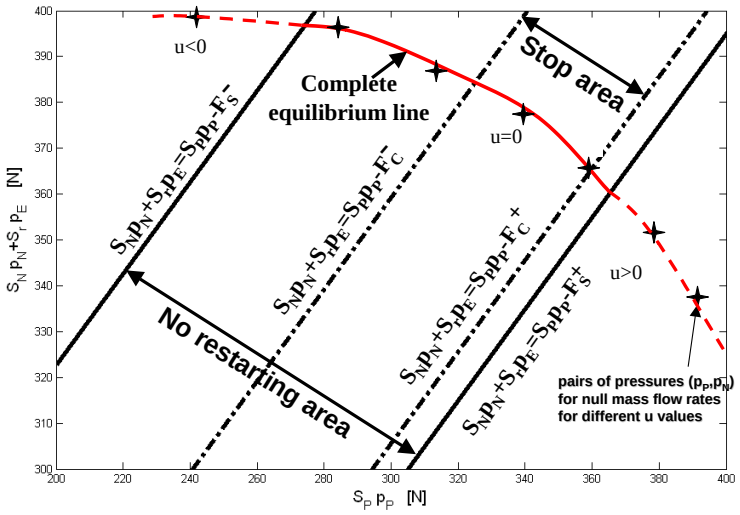

Fig 7 Pressure force plane showing the dry friction areas and the complete equilibrium line.

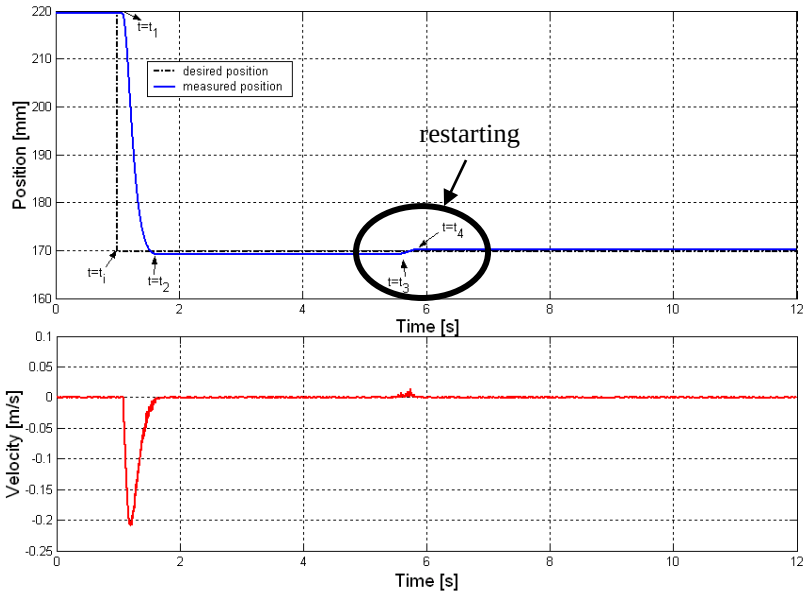

a/ Measured and desired position and velocity time evolutions

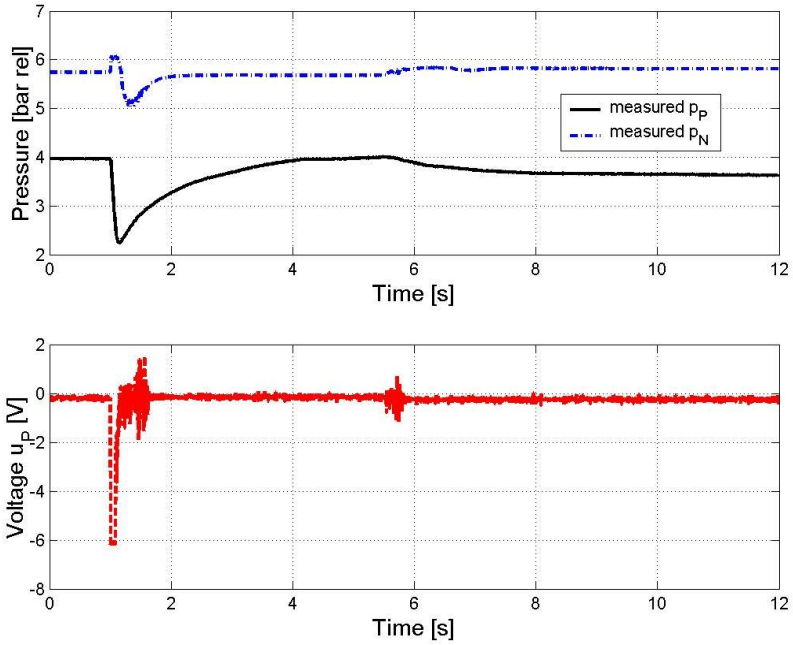

b/ Pressures and servo-distributors control input time evolutions

Fig 8 Example of experimental results with a restarting phenomenon

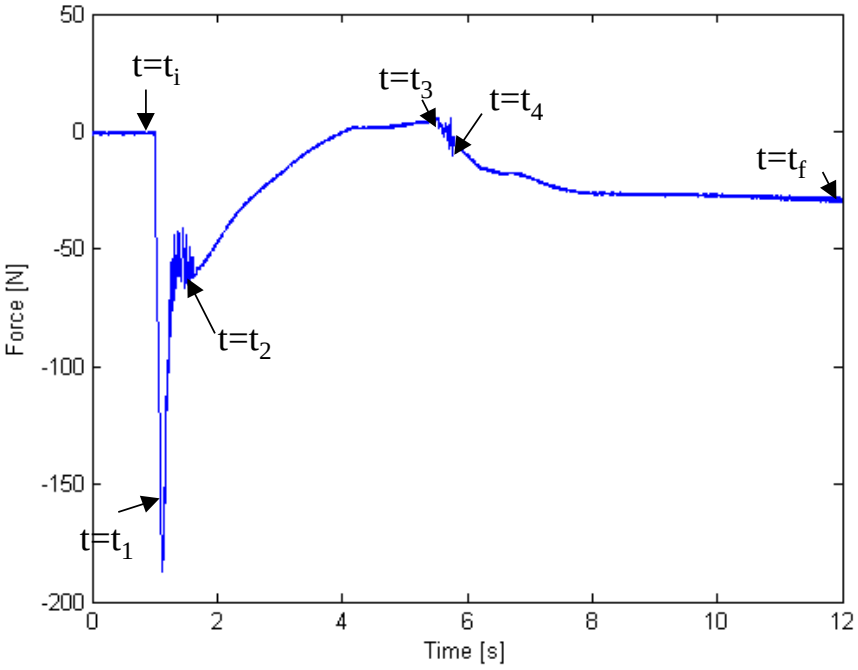

Fig 9 Estimated total pressure force time evolution

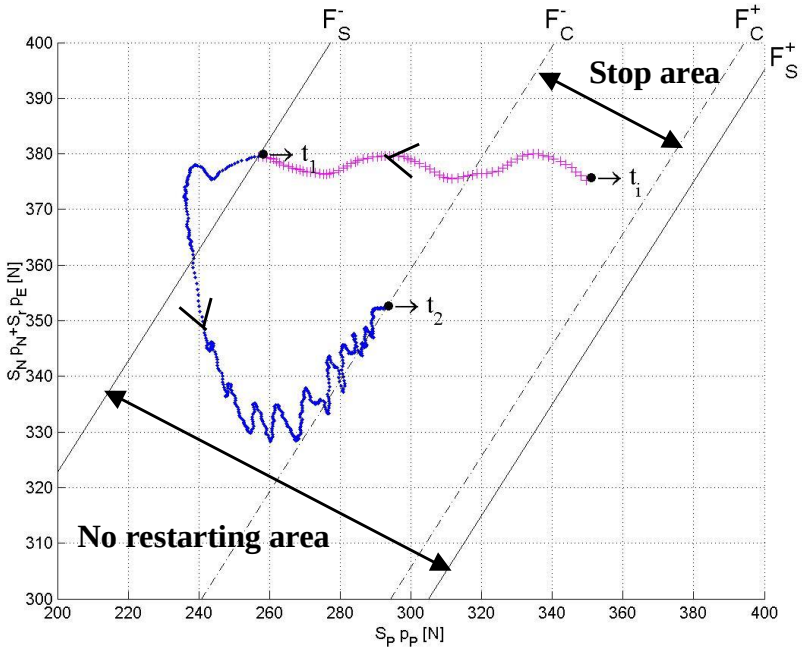

Fig 10 Analysis of the restarting phenomenon in the $\left(S_P p_P, S_N p_N + S_r p_E\right)$ plane from t_i to t_2

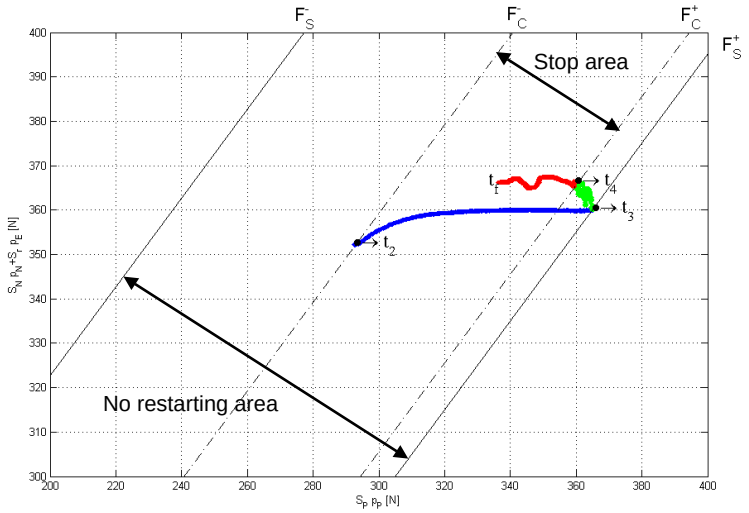

Fig 11 Analysis of the restarting phenomenon in the $\left(S_P p_P, S_N p_N + S_r p_E\right)$ plane from t2 to tf

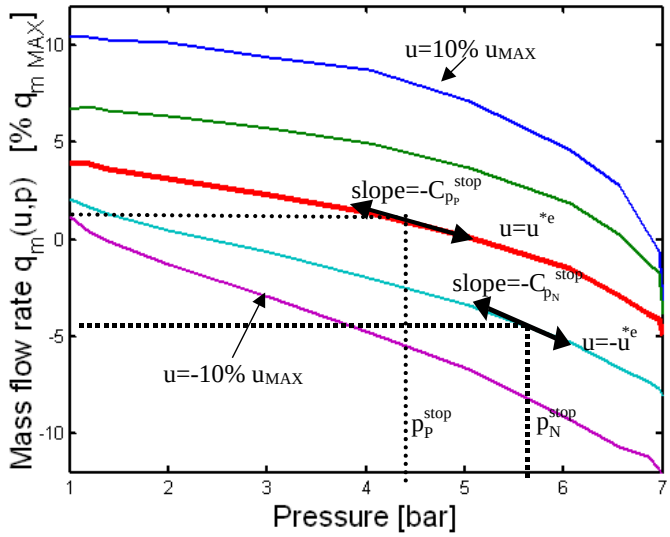

Fig 12 Experimental mass flow rate characteristics for small control signal values

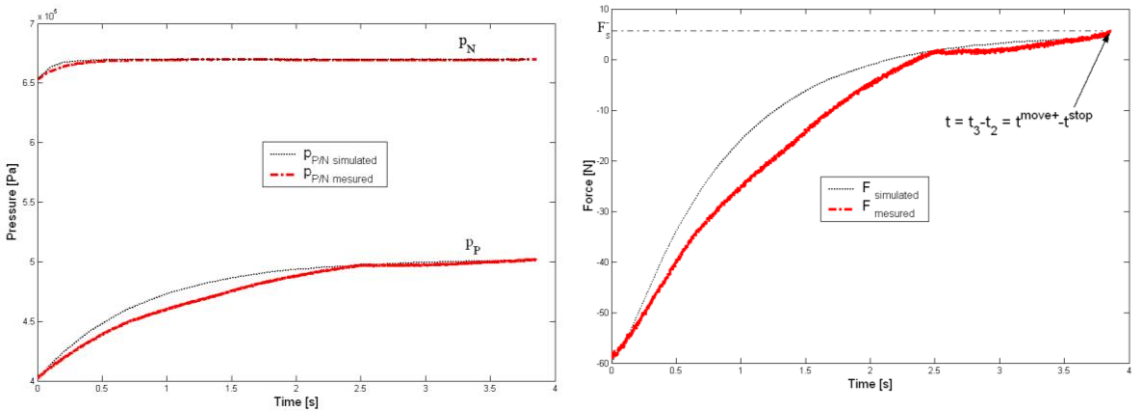

a/ Pressure evolutions **b/ Force evolution (Eq. (14))**

Fig 13 Simulated and experimental evolution during the mechanical partial equilibrium after the first stop